Temperature Distribution of a Low Temperature Heat Pipe with Multiple Heaters for Electronic Cooling

Hong-Koo Noh and Kyu-Sub Song

CONTENTS

NOMENCLATURE

I. INTRODUCTION

II. MATHEMATICAL FORMULATION AND MODELING

III. NUMERICAL PROCEDURE

IV. RESULTS AND DISCUSSIONS

V. CONCLUSIONS

REFERENCES

ABSTRACT

A numerical study has been performed to predict the characteristics on the transient operation of the heat pipe with multiple heaters for electronic cooling . The model of the heat pipe was composed of the evaporator section with four heaters, insulated transport section, and the condensor section with a conductor which is cooled with uniform heat flux condition to surrounding. The governing equations and the boundary conditions were solved by the generalized PHOENICS computational code employing the finite volume method. Two test cases are investigated in present study; Case 1 indicates that the 1st and 2nd heaters among four heating sources are heated off, while the 3rd and 4th heaters are heated on. Case 2 is the inverse situation switched from heating location of Case 1. The results show that the transient time to reach the steady state is shorter for Case 1 than for Case 2. Especially, the temperature difference of the heater during switching operation is relatively small compared to the maximum all- owable operating temperature difference in electronic system. Hence, it is predicted that the heat pipe in present study operates with thermally good reliability even for switching the heaters.

NOMENCLATURE

A : Area [m^2]
c_p : Specific heat [J/(kg·K)]
h_{fg}: Latent heat [kJ/kg]
k : Thermal conductivity [W/(m·K)]
$\dot{m}$: Mass rate [kg/s]
p : Pressure [N/m^2]
$\dot{q}$: Aeat generated per unit volume [W/m^3]
Q : Heat input [W]
R : Gas constant [N·m/(kg·K)]
Re : Reynolds number
T : Temperature [°C]
v, w : r, z-direction velocity components [m/s]
ρ : Density [kg/m^3]
μ : Viscosity [kg/(m·s)]
ν : Dynamic viscosity [m^2/s]
φ : Porosity

Subscripts

eff : Effective
h : Heater
i : Interface of vapor-wick
ℓ : Water with the liquid phase
o : Reference value or outer wall of the heat pipe
s : Screen wick
v : Vapor
w : Heat pipe wall

I. INTRODUCTION

Since the heat pipe was invented by Grover *et al.* [1], it has been applied to various fields of industry. Because the heat pipe does not need any external power to transport heat, it has been used as a cooling device for electronic system, in which several components are generally arranged in a column or a row. Conventionally, heat pipe has been installed on each heater individually. However recently, only one heat pipe may be installed on multiple heaters [2], [3]. In case of switching electronic system, inactive heaters are turned on simultaneously when active heaters are turned off. Consequently, the heat pipe with multiple heaters should experience the transient operation. During the transient operation, the failure rate of electronic components which are sensitive to temperature would be increased so that the life-time of electronic components become shorter. To affirm the thermal reliability of electronic components in the transient state, the maximum allowable operating temperature difference ($\Delta T_{\max}$) of electronic components should be kept within 55°C [4]. It is also recommended that the time to reach the steady state should be shorter to confirm the thermal stability of the heat pipe.

Many studies for heat pipe with multiple heat sources have been performed by Faghri *et al.* [5]-[8] Chen and Faghri [5] investigated the behavior of heat pipe with two heat sources. Faghri and Buchko [6] studied the dry-out condition of the heat pipe with four heat sources. Faghri *et al.* [7],[8] performed the experiments for a sodium/stainless heat pipe with four heat sources to investigate the behavior of frozen startup. In reviews of above literature, researches were mostly limited to fixed multiple heat sources and could not even cover the instantaneous switching of heaters on the heat pipe. Recently, Park and Lee [9] reported the numerical results of ideal switching operation in a high-temperature heat pipe with single heat source. Due to single heat source and high operating temperature, their results are not be directly applicable to electronic system with multiple heat sources.

Since there is few study on switching transient operation of the heat pipe with multiple heaters, using mathematical formulation and modeling of conventional study, the objective in present study is to obtain the practical results by investigating the characteristics of thermal behavior within the heat pipe with multiple heaters when the instantaneous switching operation arises.

II. MATHEMATICAL FORMULATION AND MODELING

1. Heat Pipe Model

The heat pipe configuration and coordinate system modeled in present study are presented in Fig. 1. The heat pipe of a length of L consists of a evaporator section, a transport section and a condenser section. As shown in Fig. 1, four ring-shaped heaters (heater 1, heater 2, heater 3, and heater 4) of L_1 length are installed with L_2 spacing in the evaporator section. A ring-shaped insulator of L_t length is installed in the transport section and a ring-shaped conductor of L_c length is installed in the condenser section. It is assumed that all the heaters, wall of the heat pipe, and the conductor are made of copper, as well as the wick is made of copper mesh. The vapor space in the heat pipe is assumed to be filled with working fluid, water in the vapor phase. In the radial direction, there are four regions separated: the vapor region of R_v from the center of the heat pipe, the wick region of R_w, the wall region of R_o, and the sheath region of R_h. The sheath region consists of heaters, insulators and a conductor. All external surfaces except the condenser section in the sheath region are assumed to be insulated with insulation material. The working fluid is assumed to be the liquid phase in the wick region and the vapor phase in the vapor space. It is balanced with thermodynamically equilibrium state. Once the heaters on the evaporator are heated, the working fluid in the wick region is vaporized to the vapor space and the vapor flows to the condenser region. In the condenser region, after the vapor release latent heat to the environment through the outer surface of the conductor, it returns to the wick region with the saturated liquid phase. As preliminarily studied, the non-Darcian effects and the secondary flow effects on the maximum heat removal capability were investigated for the heat pipe model of the present study. It was found that the non-Darcian effects and the secondary flow effects on the maximum heat removal capability were infinitesimal due to the long length and the small diameter of

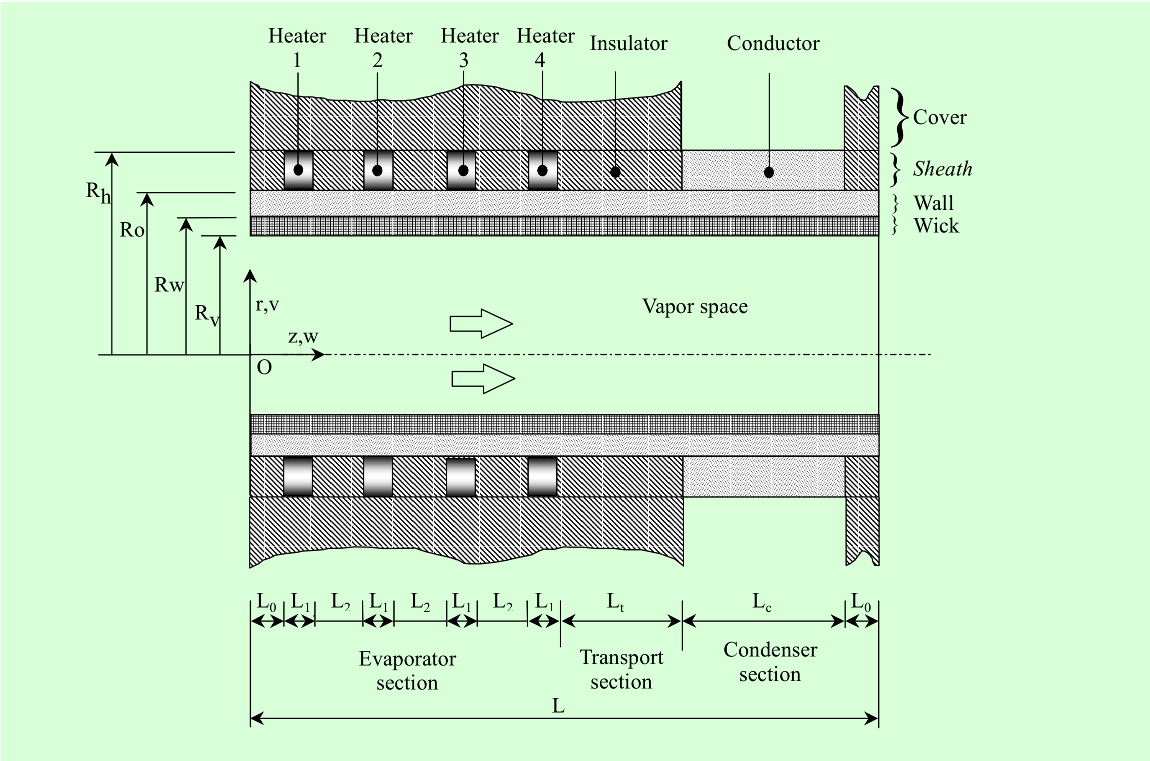

Fig. 1. Heat pipe with multiple heaters in present study.

the heat pipe model in the present study, as presented above.

2. Governing Equations

The governing equations in the present study was set up on the basis of mathematical modeling in the study of Faghri and Buchko [6]. The governing equations for the heat pipe model of Fig. 1 would be separately described in the vapor flow, wick, wall, and sheath region as follows.

A. Vapor Flow Region

From the experimental results of Bowman and Hitchcock [10], it was reported that the vapor flow in the evaporator region was always laminar and the vapor flow in the condenser region could be considered as laminar if the Reynolds number, whose characteristic length is the inner radius of the heat pipe, is less than 2000. In present numerical study, the vapor flow was assumed to be laminar along the entire tube since the Reynolds number of the vapor flow was about 1000. In addition, Dunn and Reay [2] reported that the effects of compressibility must be considered in the vapor flow of the heat pipe if Mach number in the heat pipe is higher than 0.3. Since Mach number is below 0.004 in present study, the vapor flow is incompressible flow. Accordingly, the mass, momentum, and energy equations in the vapor region are described with the 2-dimensional transient incompressible laminar flow in the axi-sysmmetric cylindrical coordinate as follows:

$$\frac{\partial \rho}{\partial t} + \frac{1}{r}\frac{\partial}{\partial r}(\rho r v) + \frac{\partial}{\partial z}(\rho w) = 0 \tag{29}$$

$$\frac{\partial}{\partial t}(\rho v) + \frac{1}{r}\frac{\partial}{\partial r}(\rho r v^2) + \frac{\partial}{\partial z}(\rho v w) = -\frac{\partial p}{\partial r} + \mu\left[\frac{\partial}{\partial r}\left(\frac{1}{r}\frac{\partial}{\partial r}(rv)\right) + \frac{\partial^2 v}{\partial z^2}\right] \tag{30}$$

$$\frac{\partial}{\partial t}(\rho w) + \frac{1}{r}\frac{\partial}{\partial r}(\rho r v w) + \frac{\partial}{\partial z}(\rho w^2) = -\frac{\partial p}{\partial z} + \mu\left[\frac{\partial}{\partial r}\left(\frac{1}{r}\frac{\partial}{\partial r}(rw)\right) + \frac{\partial^2 w}{\partial z^2}\right] \tag{31}$$

$$\rho c_p\left(\frac{\partial T}{\partial t} + v\frac{\partial T}{\partial r} + w\frac{\partial T}{\partial z}\right) = k\left[\frac{1}{r}\frac{\partial}{\partial r}\left(r\frac{\partial T}{\partial r}\right) + \frac{\partial^2 T}{\partial z^2}\right], \tag{32}$$

where ρ, μ, c_p, and k is density, viscosity, specific heat, and thermal conductivity of vapor, respectively.

B. Wick Region

Cao and Faghri [11] presented that the liquid flow in the wick region had negligible effects on the temperature distribution in the heat pipe when the liquid flow was very small. The liquid flow in present study was so very small that the magnitude of velocity vectors in the wick region was calculated below 4×10^{-5} m/s. Therefore, the liquid flow in the wick region was ignored in the present study. Hence, energy equation considering only pure conduction of wick and water in the wick region is

$$(\rho c_p)_{eff}\frac{\partial T}{\partial t} = k_{eff}\left[\frac{1}{r}\frac{\partial}{\partial r}\left(r\frac{\partial T}{\partial r}\right) + \frac{\partial^2 T}{\partial z^2}\right] \tag{33}$$

In (5), the effective heat capacity $(\rho c_p)_{eff}$ is the value obtained from (6) [11]:

$$(\rho c_p)_{eff} = \varphi \rho_\ell c_{p\ell} + (1-\varphi)\rho_s c_{ps}, \tag{34}$$

where φ means the wick porosity in the heat pipe. Subscript ℓ and s mean water in the liquid phase and screen mesh in the wick, respectively. Generally, effective thermal conductivity k_{eff} in (5) is determined from the material and type of the wick. In present study, effective thermal conductivity is obtained from the following (7) under the assumption that the wick was composed of wrapped screen mesh [11]:

$$k_{eff} = \frac{k_\ell[(k_\ell + k_s) - (1-\varphi)(k_\ell - k_s)]}{[(k_\ell + k_s) + (1-\varphi)(k_\ell - k_s)]}. \tag{35}$$

C. Wall Region

The heat through the heat pipe wall is transferred purely by conduction. The corresponding energy equation is

$$(\rho c_p)_w\frac{\partial T}{\partial t} = k_w\left[\frac{1}{r}\frac{\partial}{\partial r}\left(r\frac{\partial T}{\partial r}\right) + \frac{\partial^2 T}{\partial z^2}\right], \tag{36}$$

where subscript w means the wall of the heat pipe.

D. Sheath Region

The sheath region consists of the heater sections, the adiabatic sections, and the conductor section. Heat transfer through the sheath region is purely by conduction except the adiabatic sections. The energy equation in the conductor section is the same as shown in (8). The energy equation in the heater sections including the heat generation is

$$(\rho c_p)_h \frac{\partial T}{\partial t} = k_h \left[\frac{1}{r}\frac{\partial}{\partial r}\left(r\frac{\partial T}{\partial r}\right) + \frac{\partial^2 T}{\partial z^2}\right] + \dot{q}, \quad (37)$$

where subscript h means heater and source term $\dot{q}$ is the volumetric heat generation in heaters.

3. Boundary Conditions

To solve above equations for the heat pipe, boundary conditions should be given at end caps of the heat pipe, centerline of heat pipe, vapor-wick interface, wick-wall interface, and sheath-cover interface.

At end caps of the heat pipe, no-slip and adiabatic conditions are given as

$$v = w = 0, \quad \frac{\partial T}{\partial z} = 0 \ ; \ z = 0 \text{ and } L. \quad (38)$$

Since the heat pipe is symmetric along the centerline, the following conditions maybe set at the centerline of the heat pipe:

$$\frac{\partial w}{\partial r} = 0, \ v = 0, \ \frac{\partial T}{\partial r} = 0 \ ; \ \text{ at } r = 0 \ . \quad (39)$$

At the vapor-wick interface, the temperature is assumed to be the saturation temperature corresponding to the interface pressure during transient operation of the heat pipe. Thus, by applying the Clasius-Clapeyron relations, the saturation temperature can be determined by

$$T = \frac{1}{(1/T_o) - (R/h_{fg})\ln(p_v/p_o)} \ ; \ \text{ at } r = R_v, \ (12)$$

where T_o, p_o, p_v, R and h_{fg} are the reference saturation temperature, the reference saturation pressure, vapor pressure at the vapor-wick interface, gas constant and latent heat of water, respectively. Besides, the latent heat occurred at the liquid-wick interface is considered. Using energy balance at the vapor-wick interface, the boundary condition for velocity at the vapor-wick interface is defined as

$$\dot{m} = \rho v = \left(k_v \frac{\partial T_v}{\partial r} - k_{eff}\frac{\partial T_\ell}{\partial r}\right) / h_{fg},$$
$$w = 0 \text{ and } T_v = T_\ell \ ; \ \text{ at } r = R_v, \quad (13)$$

where k_v, T_v and T_ℓ are thermal conductivity of vapor, the vapor temperature and the liquid temperature in the wick, respectively. At the vapor-wick interface of the evaporator, radial velocity of the vapor, v is negative and working fluid is blown to the vapor region. At the vapor-wick interface of the condenser, v becomes positive and working fluid is sucked into the wick.

At the wick-wall interface, since the heat flux transferred from the wall is equivalent with that transferred to the wick, the boundary condition is

$$k_w \frac{\partial T_w}{\partial r} = k_{eff}\frac{\partial T_\ell}{\partial r} \text{ and } T_w = T_\ell \ ; \ \text{ at } r = R_w. \quad (14)$$

At the wall-sheath interface covered with insulator, the boundary condition is

$$\left.\frac{\partial T_w}{\partial r}\right|_{r = R_o} = 0. \quad (15)$$

At the wall-sheath interface, the heaters are stuck on the heat pipe wall with the material of thermal bond or thermal pad,

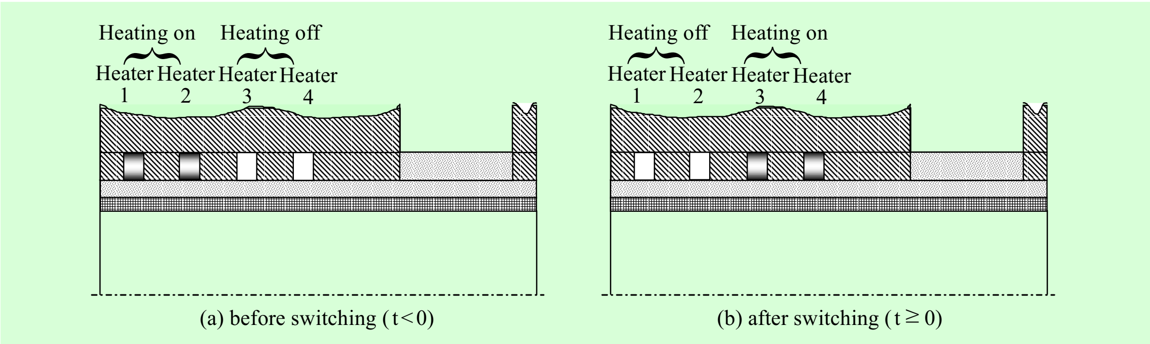

Fig. 2. Switching condition: (a) heaters 1 and 2 are heated on at $t < 0$, (b) heaters 1 and 2 are heated off and heater 3 and 4 are heated on at $t = 0$.

solidly. Therefore, disregarding thermal contact resistance at the wall-sheath interface covered with heaters and a conductor is available. The boundary condition at the wall-sheath interface is given

$$k_w \frac{\partial T_w}{\partial r} = k_c \frac{\partial T_h}{\partial r} \text{ and } T_w = T_h \; ; \quad \text{at } r = R_o, \tag{16}$$

where subscript c means heater or conductor and T_h is the sheath temperature.

Because the sheath-cover interfaces are insulated in the heater and insulator sections, the boundary condition is determined by

$$\left. \frac{\partial T_h}{\partial r} \right|_{r = R_h} = 0. \tag{17}$$

On the other hand, the boundary condition at the sheath-cover interface in the conductor section is given with uniform heat flux as

$$\left. k_c \frac{\partial T_h}{\partial r} \right|_{r = R_h} = Q/A, \tag{18}$$

where Q is total heat to be applied to the heat pipe from heaters, and A is the surface area of a conductor.

4. Initial Condition

Figure 2 shows instantaneous switching situation of heat sources from heaters 1 and 2 to heaters 3 and 4. Before the switching of heat sources, heat pipe is operating under the steady state with heaters 1 and 2 heated on as shown in Fig. 2(a). The values of dependent variables (p, v, w, and T) obtained from the calculation for steady state are given as the initial conditions for the transient calculation. Besides, the initial conditions of switching situation from heaters 3 and 4 to heaters 1 and 2 are similarly given as mentioned above.

III. NUMERICAL PROCEDURE

The governing equations and boundary conditions were solved by the generalized PHOENICS computational code employing the finite volume method [12]. The upwind scheme and Jacobi's point-by-point method for the solution of momentum equation were used. Thermal conductivity at the interfaces of vapor-wick, wick-wall and wall-sheath was taken by the harmonic averaging method. Preliminarily, three kinds of the grid number were tried about 42 (axial) $\times$ 25 (radial), 47 (axial) $\times$ 30 (radial) and 52 (axial) $\times$ 35 (radial), respectively. The numerical results on these three kinds of the grid number had a good agreement within error of 0.02%. Therefore, for the calculation domains, the number of grids was chosen as 47 (axial) $\times$ 30 (radial). Under-relaxation method was introduced in iteration process. The converged solution was obtained with the criterion that the residuals of dependent variables were less than 10^{-9} between successive iterations. The calculation was conducted on a PC586 and about 30 minutes were taken to run each case.

IV. RESULTS AND DISCUSSIONS

1. Numerical Verification

The verification for present numerical calculation was preliminary performed. For calculation, each length of the heat pipe is $L_0 = 0.02$ m, $L_1 = 0.0635$ m, $L_2 = 0.0735$ m, $L_t = 0.18$ m, $L_c = 0.3$ m, $L = 1$ m, $R_v = 0.01025$ m, $R_w = 0.011$ m, $R_o = 0.0127$ m and $R_h = 0.0144$ m. Heaters 1, 2, 3, and 4 had heat dissipation of 20 W each. The cooling condition at condenser section was set to be uniform heat flux. Figure 3 shows the temperature profiles at the wall-sheath interface along the axial coordinates to compare with the study of Faghri and Buchko [6]. As shown in figure, the temperatures at wall-sheath interface in present study is about 1.2°C lower in the evaporator section and about 1.4°C higher in the condenser section than those of Faghri and Buchko [6]. This inconsistency of temperatures in the evaporator and condenser sections seems to arise from the ignorance of fluid flow in the wick in present study. However, the temperatures in the transport section have a good agreement with those of Faghri and Buchko [6]. Also, the temperature differences in the evaporator and condenser sections are negligibly small. Thus, one can accept the present modeling to predict the operation of the heat pipe with multiple heaters.

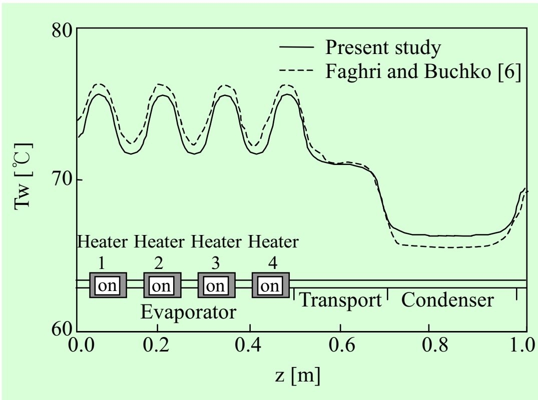

Fig. 3. Comparison of temperatures at wall-sheath interface along the axial location.

2. Test Cases

Two test cases of the present study are summarized in Table 1. As shown in Fig. 2, Case 1 is that the heaters 1 and 2 are turned off simultaneously from 20 W to 0 W. At the same time, the heaters 3 and 4 are heated simultaneously from 0 W to 20 W. On the contrary, Case 2 is the inverse situation of Case 1. Thermal properties of the heat pipe at 60°C are used in present investigation and the detailed properties are as shown in Table 2.

Table 1. Test cases for present study.

(unit: W)

Case	Heater 1	Heater 2	Heater 3	Heater 4
1	$20 \rightarrow^* 0$	$20 \rightarrow 0$	$0 \rightarrow 20$	$0 \rightarrow 20$
2	$0 \rightarrow 20$	$0 \rightarrow 20$	$20 \rightarrow 0$	$20 \rightarrow 0$

∗ The arrow means that the power of heater is changed instantaneously at $t = 0$.

3. Transient Operation for Switching Heaters

The dimension of the heat pipe was chosen considering the dimension of electronic system. The length and diameter of present heat pipe are 0.45 m and 0.0158 m, respectively. The details for each length in Fig. 1 are $L_0 = 0.01$ m, $L_1 = 0.04$ m, $L_2 = 0.025$ m, $L_t = 0.055$ m, $L_c = 0.14$ m, $L = 0.45$ m, $R_v = 0.0059$ m, $R_w = 0.0069$ m, $R_o = 0.0079$ m and $R_h = 0.01$ m. Regarding these dimension of the heat pipe, the behaviors of the heat pipe in two cases during the transition were compared with transient flow in the vapor space and transient temperature at the wall of the heat pipe.

Table 2. Summary of the heat pipe model.

Wall		Material : Pure copper Density, ρ_s = 8914.8 kg/m^3 Specific heat, C_{ps} = 389.3 J/(kg·K) Thermal conductivity, k_s = 398.4 W/(m·K)
Wick		Material : Copper* 100 mesh screen Diameter of wire, d = 0.1 mm Width of opening, w = 0.16 mm Thickness of a layer, t = 0.23 mm Porosity, φ^{**} = 0.737
Working fluid	Liquid	Latent heat, h_{fg} = 2.3584×10^6 J/kg Density, ρ_ℓ = 983.28 kg/m^3 Viscosity, μ_ℓ = 4630×10^{-7} kg/(m·s) Thermal conductivity, k_ℓ = 0.653W/(m K) Specific heat, $C_{p\ell}$ = 4185 J/(kg·K) Surface tension, σ = 66.07×10^{-3} N/m
	Vapor	Gas constant, R = 459 J/(kg·K) Density, ρ_v = 0.1302 kg/m^3 Viscosity, μ_v = 105.0×10^{-7} kg/(m·s) Thermal conductivity, k_v = 0.0216 W/(m·K) Specific heat, C_{pv} = 1924 J/(kg·K)

* The density, specific heat and thermal conductivity of the wick and the heaters are the same as those of the wall.

** $\varphi = 1 - \frac{\pi AB}{2(1+A)}$, $A = d/w$, $B = d/t$ by Chang [14]

Above all, to visualize the flow in the vapor space of the heat pipe during switching heaters, transient velocity distributions are shown in Fig. 4 for Case 1. In Fig. 4(a) at the initial state, the flow in the region of heaters 1 and 2 is downward right-handed. In Fig. 4(b) at $t = 10$ s and Fig. 4(c) at $t = 30$s, the flow in the region of heaters 1 and 2 is getting smaller. In Fig. 4(d) at

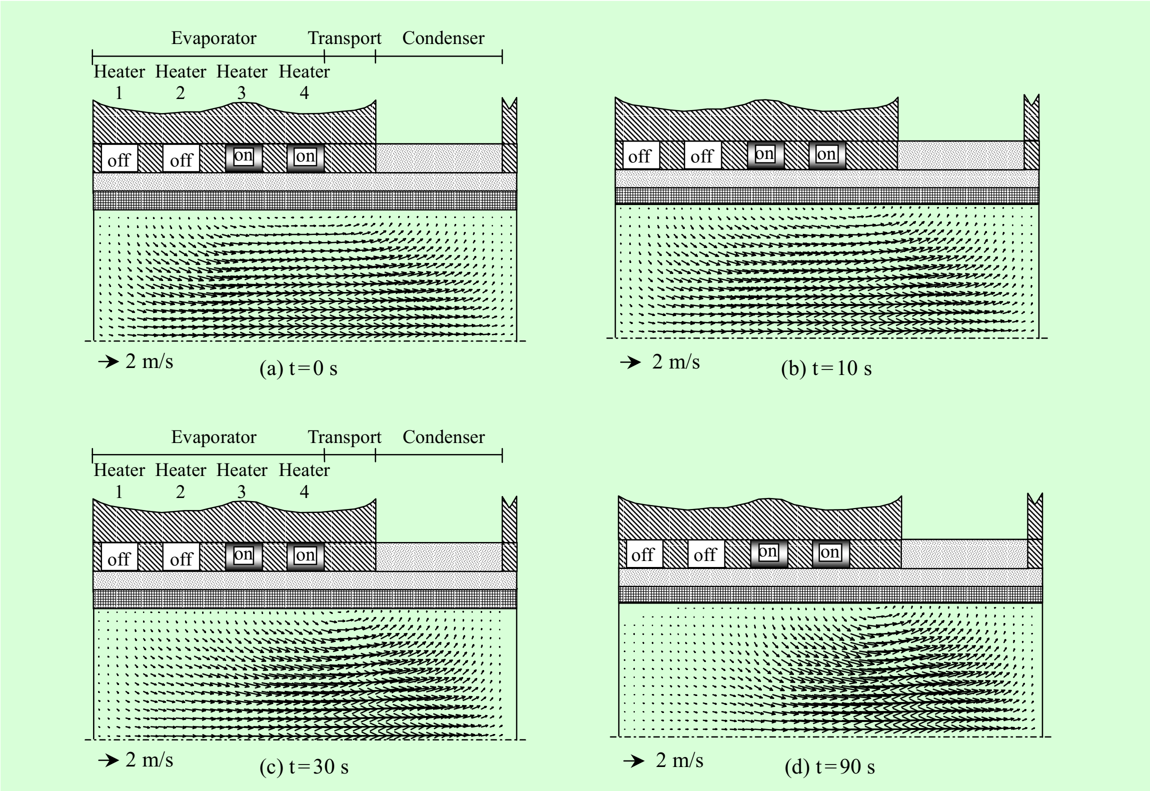

Fig. 4. Transient velocity profile in vapor space for case 1.

$t = 90$ s, it becomes very small. On the other hand, In Fig. 4(a) at the initial state, the flow in the region of heater 3 and 4 is wholly right-handed. In Fig. 4(b) at $t = 10$ s and Fig. 4(c) at $t = 30$ s, the flow in the region of heater 3 and 4 becomes more and more downward. In Fig. 4(d) at $t = 90$ s, it is downward right-handed. The downward right-handed flow during the transition moves from the region of heaters 1 and 2 to the region of heaters 3 and 4 as heat source moves from heaters 1 and 2 to heaters 3 and 4 for Case 1. Meanwhile, the flow in the transport and condenser sections remains unchanged during the transition. Additionally, it can be confirmed that the flow is incompressible because all velocities in the vapor space are calculated less than 1.8 m/s (corresponding to Mach number 0.004) during the transition. Since there is no more change for the flow in the heat pipe after $t = 90$ s for Case 1, the transient time to reach the steady state is about 90 seconds for Case 1.

Transient velocity distributions for Case 2 are shown in Fig. 5. As shown in this Figure, during the transition, entire trend of the flow change for Case 2 is inverse against that for Case 1. Besides, the transient time to reach the steady state

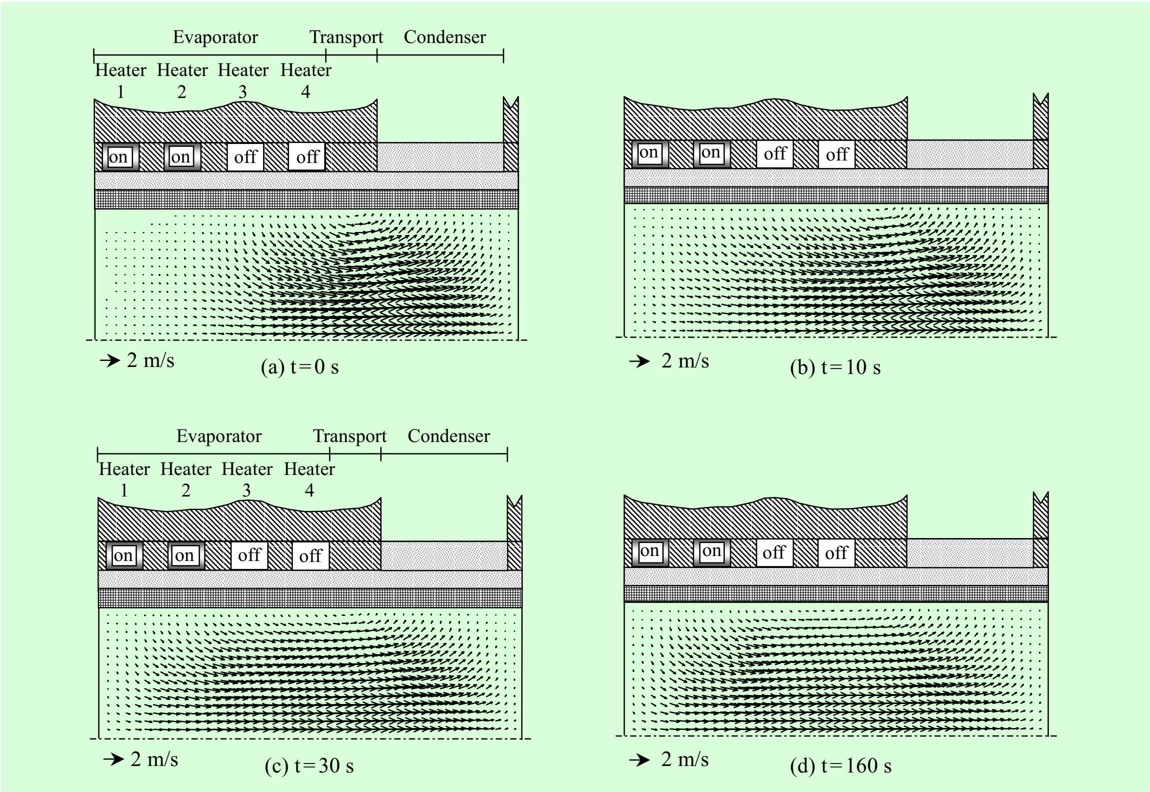

Fig. 5. Transient velocity profile in vapor space for case 2.

is about 160 seconds for Case 2. This is 70 seconds longer than that for Case 1. In other words, the transient time is shorter in situation that the heaters located far from the condenser section are turned off.

To investigate the location and the quantity of the evaporation and condensation, the radial velocity components v at the vapor-wick interface for two cases are shown in Fig. 6. In this figure, the radial velocity component v is negative for the evaporation and positive for the condensation as shown in the coordinates of Fig. 1. Besides, the bigger radial velocity component means more evaporation or condensation. In Fig. 6(a) for Case 1, at $t = 0$ s (initial state), there is the evaporation at the evaporator section, while there is the condensation at the transport and condenser sections. There is great evaporation at heaters 1 and 2 in the evaporator section, while there is small evaporation at heaters 3 and 4. During the transition from initial state, the evaporation at heaters 1 and 2 decreases, while the evaporation at heaters 3 and 4 increases since heaters 1 and 2 are heated off and heaters 3 and 4 are heated on. During the transition, in the transport section, the starting location of the condensation moves slightly to the direction of

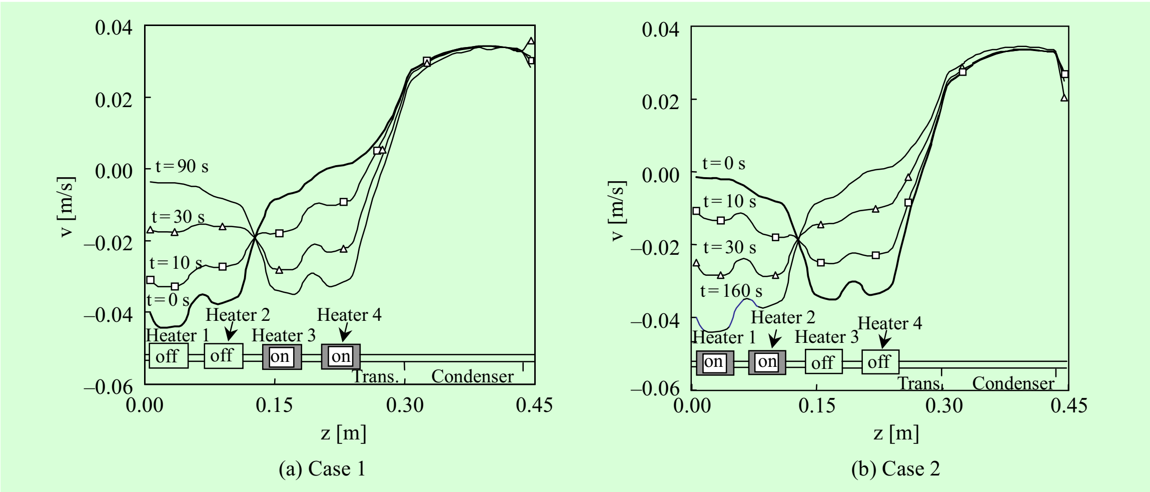

Fig. 6. Transient radial velocities at vapor-wick interface along the axial location.

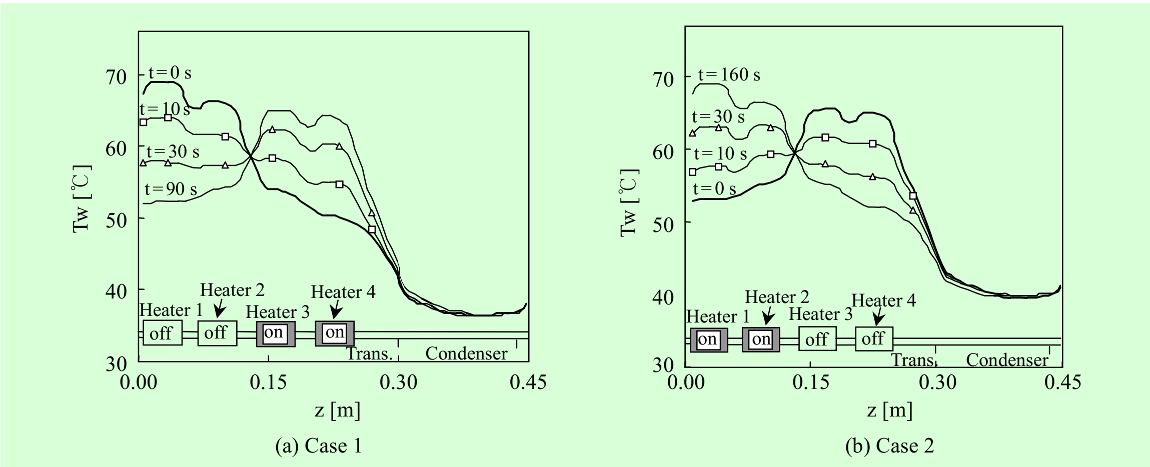

Fig. 7. Transient temperatures at wall-sheath interface along the axial location.

the condenser section. During the transition, in the condenser section, the constant condensation is observed. In Fig. 6(b) for Case 2 opposite to Case 1, during the transition from initial state, the evaporation at heaters 1 and 2 increases, while the evaporation at heaters 3 and 4 decreases since heaters 1 and 2 are heated on and heaters 3 and 4 are heated off. During the transition, in the transport section, the starting location of the condensation moves slightly to the direction of the evaporator section.

As mentioned in the introduction, the temperature difference of electronic components during the transition should be kept within 55°C. To investigate this, the transient temperatures at wall-sheath interface for two cases are shown in Fig. 7. In Fig. 7(a) for Case 1, at $t = 0$ s, the temperatures at wall-sheath interface are high at the heater 1, gradually decreasing at the heater 2, 3 and 4, low in the condenser section. During the transition process from initial state, the temperatures at heaters 1 and 2 gradually decrease, while the temperatures at heater 3 and 4 gradually increase since heaters 1 and 2 are heated off and heaters 3 and 4 are heated on. During the transition, the temperatures in the transport section slightly increase, while those in the condenser section remains unchanged. In Fig. 7(b) for Case 2, during the transition, the temperatures at heaters 1 and 2 gradually increase, while the temperatures at heater 3 and 4 gradually decrease since heater 1 and 2 are heated on and heaters 3 and 4 are heated off. In both cases, since the temperatures at the wall-sheath interface in the condenser section remain unchanged during the transition, it is found that the heat pipe operates with no thermal change in the condenser section even during switching heaters. In both cases, the temperature difference between the switched-on-heater and switched-off-heater sections during switching operation is maximum 18°C, which is relatively small compared to the maximum allowable operating temperature difference of 55°C in electronic system. Hence, it is predicted that the heat pipe for two cases operate with thermally good reliability in present study.

The temperatures change for four heaters during the transition are typically investigated for Case 1, in Fig. 8. As shown in this figure, the temperatures of each heater reach to 90% of the whole temperature change within 45 seconds after the switching of the heaters, decreasing or increasing exponentially during the transition. Therefore, the heat pipe in range of heat load given in present study attains to mostly thermal response within 50% of the whole transient time.

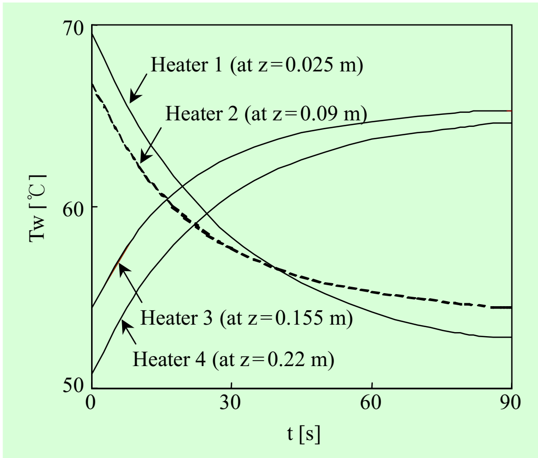

Fig. 8. Transient temperatures at wall-sheath interface in four heaters for case 1.

V. CONCLUSIONS

A numerical study to predict the characteristics on the transient switching operation of the heat pipe with multiple heaters for electronic cooling is performed. As a result, the following conclusions are obtained.

(1) The transient times to reach the steady state are 90 seconds for Case 1, and

160 seconds for Case 2, respectively. The transient time for Case1 is shorter by 70 seconds compared with Case 2. Thus, the transient time is shorter in situation that the heaters located far from the condenser section are turned off.

(2) For the heater heat dissipation of 20 W, the temperature difference between the switched-on-heater and switched-off-heater sections during switching operation is relatively small compared to the maximum allowable operating temperature difference in electronic system. Hence, it is predicted that the heat pipe for two cases operate with thermally good reliability in range of heat load given in present study even for the switching of the heaters.

(3) The temperatures of each heater reach to 90% of the whole temperature change within 50% of the whole transient time, decreasing or increasing exponentially during the transition.

REFERENCES

[1] G. Grover, T.P. Cotter, and G.F. Erikson, "Structures of Very High Thermal Conductance," *J. Appl. Physics*, Vol. 6, 1964, pp. 1990–1991.

[2] P.D. Dunn, and D.A. Reay, *Heat Pipes*, 4th ed., Pergamon, New York, 1994, pp. 120–250.

[3] A. Faghri, *Heat Pipe Science and Technology, Taylor & Francis*, Washington, DC, 1995, pp. 180–220.

[4] W.T. Kim, "Thermal Management and Cooling Technology of Electronic Packaging in the ISDN Communications," *KSME*, Vol. 36, No. 4, 1996, pp. 351–364.

[5] M.M. Chen, and A. Faghri, "An Analysis of the Vapor Flow and the Heat Conduction through the Liquid-Wick and Pipe Wall in a Heat Pipe with Single or Multiple Heat Source," *Int'l Journal of Heat Mass Transfer*, Vol. 33, No. 9, 1990, pp. 1945–1955.

[6] A. Faghri, and M. Buchko, "Experimental and Numerical Analysis of Low-Temperature Heat Pipes with Multiple Heat Sources," *Journal of Heat Transfer*, Vol. 113, 1991, pp. 728–734.

[7] A. Faghri, M. Buchko, and Y. Cao, "A Study of High-Temperature Heat Pipes with Multiple Heat Sources and Sinks: Part I–Experimental Methodology and Frozen Startup Profiles," *Journal of Heat Transfer*, Vol. 113, 1991, pp. 1003–1009.

[8] A. Faghri, M. Buchko, and Y. Cao, "A Study of High-Temperature Heat Pipes with Multiple Heat Sources and Sinks: Part II–Analysis of Continuum Transient and Steady State Experimental Data with Numerical Predictions," *Journal of Heat Transfer*, Vol. 113, 1991, pp. 1010–1016.

[9] J.H. Park, and J.H. Lee, "A Numerical Study on the Heat Pipe with Switched Heat Source and Sink for Space Application," *Proc. of the KSME 1996 Spring Annual Meeting B* 1996.

[10] W.J. Bowman, and J. Hitchcock, "Transient Compressible Heat-Pipe Vapor Dynamics," *Proc. of 25th ASME National Heat Transfer Conference*, Vol. 1, 1988, pp. 361–365.

[11] Y. Cao, and A. Faghri, "Transient Two-Dimensional Compressible Analysis for High Temperature Heat Pipes with a Pulsed Heat Input," *Numerical Heat Transfer*, Part A, Vol. 18, 1990, pp. 483–502.

[12] H.I. Rosten, and D.B. Spalding, Phoenics Training Course Notes CHAM TR/300, CHAM 1990.

[13] A. Faghri, and M.M. Chen, "A Numerical Analysis of the Effects of Conjugate Heat Trensfer, Vapor Compressibility, and Vicous Dissipation in Heat Pipes," *Numerical Heat Transfer*, Part A, Vol. 16, 1989, pp. 389–405.

[14] W.S. Chang, "Porosity and Effective Thermal Conductivity of Wire Screens," *Journal of Heat Transfer,* Vol. 112, 1990, pp. 5–9.

[15] S.J. Kim, *Air Cooling Technology for Electronic Equipment*, CRC Press, 1996.

Hong-Koo Noh received his B.E. degree from Hangkong University, Seoul, Korea in 1985, and received M.E. and Ph.D. in mechanical engineering from Hanyang University, Seoul, Korea in 1989 and 1998, respectively. He has worked for ETRI as a senior researcher. He is responsible for the thermal management of electronic equipment in ETRI. He has recently joined in the project associated with the thermal management in the telecommunication building. He is an active member of the KSME, where he has published over 10 technical papers covering the range of heat transfer problems for the electronics cooling.

Kyu-Sub Song received his B.E. degree in mechanical enginneering from Pusan National University, Pusan, Korea in 1981, and received M.E. from Chonbuk National University, Chonju, Korea in 1993. He has worked for ETRI as a project manager. He is responsible for the structure design of electronic equipment in ETRI. He has recently joined in the project associated with the venture business support.